Structure–Property Relationships in Thermally Aged Cellulose Fibers and Paper

K. L. KATO, R. E. CAMERON

University of Cambridge, Department of Materials Science and Metallurgy, New Museums Site, Pembroke Street, Cambridge, CB2 3QZ, Great Britain

Received 24 December 1998: accepted 20 April 1999

ABSTRACT: The research presented in this paper investigates the effect of thermally accelerated aging on the submicrostructure of cellulose and attempts to relate such changes to the well-documented loss of mechanical strength in aged paper. Filter paper and ramie fibers samples were aged *in vacuo* at 160°C. Small angle X-ray scattering (SAXS) was used to study void structure within the fibers and hydration used as a structural probe. On hydration, the void radius of gyration and area decrease, while the void aspect ratio and overall void fraction increase. After aging, the wet structure more closely resembles the dry, suggesting that water cannot expand the structure to the same extent. It is postulated that increases in local ordering on aging create a structure more resistant to disruption by water. The use of additional techniques, namely Fourier transform IR spectroscopy, wide angle X-ray scattering, scanning electron microscopy (SEM), environmental SEM, and measurement of water retention value, provided additional indirect support for the postulated model. There is no direct evidence for significant crystallinity changes in aged material, suggesting that if structural rearrangements occur, they will be local in nature. There is also no evidence for the formation of covalent crosslinks or new chemical species on aging. Water retention values and wet SAXS results concur, highlighting the importance of water in the cellulose structure and the reduced capacity for water sorption in aged samples. SEM observations show that the failure mechanism in paper changes with age from fibers pull out (i.e., interfiber bond failure) to fiber failure, and wide and zero span tensile tests indicate a weakening of the fibers. These results are consistent with previous reports, and we attribute them primarily to chain scission, although the increased intrafiber bonding may have an influence on the values obtained. J Appl Polym Sci 74: 1465–1477, 1999

Key words: cellulose; thermally accelerated aging; hornification; small angle X-ray scattering; structure; voids

INTRODUCTION

Paper is a ubiquitous material whose properties over extended periods are of interest not only to the archivist seeking to preserve historical documents, but also to the electrical industry, which uses paper insulation in cables and power transformers. Much of the previous work on this subject has focused on either the chemistry and kinetics of degradation or the mechanical behavior of aged papers. The objective of this work is to explore the internal structure of the cellulose fibers as a function of aging and the relationships between this structure and mechanical properties and water interactions. One aging temperature

Correspondence to: R. E. Cameron (e-mail: rec11@cam.ac.uk).

Journal of Applied Polymer Science, Vol. 74, 1465–1477 (1999)
 CCC 0021-8995/99/061465-13

and environment is considered here. We report an investigation of their influence in a separate paper.[1]

MATERIALS

Samples of cleaned combed ramie fibers (long cellulose fibers) supplied by Fibrecrafts and Whatman No. 40 ashless filter paper (which contains cellulosic mass from cotton linters), were aged at a constant temperature of 160°C in a vacuum oven, fitted with a roughing pump giving a pressure of approximately 3–10 mbar. The times of aging were 0, 47.25, 187.75, 503.50, and 1772.25 h. Paper sample dimensions were dictated by the standard sizes used in mechanical testing: wide span samples were 150 × 25 mm, zero span samples were 90 × 15 mm. In both cases, paper samples were cut such that the long dimension was parallel to the machine direction (parallel to the preferred orientation of fibers). Samples were removed at intervals and stored in sealed plastic bags prior to testing.

The choice of aging conditions was based on the findings of previous work on thermal aging.[2–4] Aging at 160°C is likely to induce thermal degradation (but not pyrolysis) in addition to hydrolysis and oxidation, although aging *in vacuo* should restrict the degree of oxidation compared with aging in air.

EXPERIMENTAL METHOD AND DATA ANALYSIS

Small Angle X-ray Scattering

Small angle X-ray scattering (SAXS) data was collected using synchrotron radiation at Station 8.2 (quadrant detector) or Station 2.1 (area detector), at the CLRC Daresbury Laboratory in Warrington, UK. Individual exposure times of 30 s were used. Paper samples were affixed directly in the beam. An empty beam was taken as the background. Ramie samples were placed in brass cells with thin mica windows. The background in this case was an empty or water-filled cell for dry and wet samples, respectively. "Wet" samples were soaked in distilled water for at least an hour prior to exposure, and care was taken with fiber samples to ensure that interfiber spaces were water filled by using a syringe to dislodge air bubbles.

The raw SAXS data was processed to subtract background scattering, correct for variations in the detector response, normalize to the signal from an ionization chamber placed behind the sample, remove the electronically introduced "tac hole" (time-to-analogue conversion), and define the region of admissible data. The scattering angle was calibrated using wet rat tail collagen. In the case of area data, the corrected and normalized SAXS pattern was reduced to one-dimensional data by integrating meridionally across the scattering to produce equatorial slit smeared data.

The Guinier extrapolation was calculated by fitting a straight line to the first five points of experimental data plotted on ln I vs q^2 or q coordinates, depending on whether unoriented or oriented samples were used. It should be noted that the minimum value of q used in the Guinier extrapolation was 0.005 $Å^{-1}$ in ramie and 0.0115 $Å^{-1}$ in paper. This means that the results cannot be compared directly. The q range used in the extrapolation was 1.1×10^{-3} $Å^{-1}$ in ramie and 2.6×10^{-3} $Å^{-1}$ in paper.

The invariant, or scattering power of the samples, defined as

$$Q = \int_0^\infty I(q)q^2\,dq \text{ for particles}$$

$$\tilde{Q} = \int_0^\infty \tilde{I}(q)q\,dq \text{ for slit smeared data}$$

was calculated between $q = 0$ (using data extrapolated from Guinier analysis) and the upper limit of experimental data (about 0.2 $Å^{-1}$ for the paper samples). The calculated invariant will be smaller than the true invariant because of the loss of high angle information.

Assuming all samples have an equal volume and that the void edges are sharp, the invariant is proportional to a function of electron density difference $\Delta\rho$ and void fraction ϕ:

$$(\Delta\rho)^2\phi(1 - \phi)$$

The values of the invariant were renormalized to remove the density difference term. The factor c, by which the wet invariant was multiplied, was determined by calculating the quotient of the dif-

ference in electron densities of dry and wet cellulose, and is

$$c = \frac{(\Delta\rho_{dry})^2}{(\Delta\rho_{wet})^2} = \frac{(\rho_{cellulose} - \rho_{air})^2}{(\rho_{cellulose} - \rho_{water})^2} = \frac{(0.511 - 3.88 \times 10^{-5})^2}{(0.511 - 0.334)^2} = 8.3$$

where units of electron density are $e^- \cdot \mathring{A}^{-3}$. To further assist with the interpretation of the data, all values were normalized to the dry unaged material, which was arbitrarily given a value of unity. We refer to the resulting quantity as the "void fraction product" (VFP) rather than the invariant, as the values have been normalized and corrected for the difference in contrast between dry and wet samples.

The Guinier extrapolation also yields the value of intensity at zero angle from the intercept of the line. For oriented rods, the cross sectional area across the fibers perpendicular to the fibers axis S_3 can be expressed as[5]

$$S_3 = 2\pi \frac{\lim_{q\to 0}\tilde{I}(q)}{\tilde{Q}}$$

which is the limiting value of the intensity at zero scattering angle divided by the invariant multiplied by 2π. Using the area together with the radius of gyration calculated by using the Guinier extrapolation, the aspect ratio of the cross section can be calculated. If the scattering particles are assumed to be rectangular (width x, length y) in cross section, the equations for radius of gyration and cross sectional area are, respectively,

$$R_g^2 = \frac{x^2 + y^2}{12}$$

$$S_3 = xy$$

These two equations may be solved simultaneously to give expressions for x and y. The void aspect ratio is defined as the ratio of x and y.

The azimuthal (or angular) scan procedure of Ruland and co-workers[6,7] for calculating the average void length projected onto the fibers axis L_3 and the width of the angular distribution of voids to the fibers axis B_ϕ was applied to data from oriented ramie fibers. At a fixed radius in q, the intensity in a strip of constant width in q was integrated from 0° to 180°. A Lorentzian fit was then applied to yield the integrated area and height and the area divided by the height to produce the parameter B_{obs}, which is a measure of the width of the intensity curve. Using values of B_{obs} from different radii allows a plot of $(B_{obs}s)^2$ vs s^2 to be made.

$$(B_{obs}s)^2 = (B_\phi s)^2 + \left(\frac{1}{L_3}\right)^2$$

The program XFIX* was used to produce integrated intensity curves and Lorentzian fits for at least 12 angular scans for each data file. Linear least squares fitting was applied to the plots of $(B_{obs}s)^2$ vs s^2 to yield L_3 and B_ϕ.

Wide Angle X-ray Scattering

Wide angle X-ray scattering (WAXS) data were collected with a Philips $\theta - 2\theta$ diffractometer using CuK_α radiation. The X-ray generator operated at 40 kV and 25 mA. The divergent and scatter slits were 0.5° wide; the receiving slit was 0.2 mm in size. The range between 6°(2θ) and 60°(2θ) was scanned at a step size of 0.2°(2θ) and a dwell time of 12.5 s per step. Dry paper samples were mounted on an aluminium holder such that the scattering in reflection was collected.

Intensity ratios are commonly used to calculate cellulose crystallinity. All were found to give similar results from our data. The crystallinity index of Segal[8] reported here. It is expressed as

$$CI = \frac{I_{max} - I_{min}}{I_{max}}$$

where I_{max} is the height of the (002) peak and I_{min} is the height of the minimum between the (101) and ($10\bar{1}$) peaks.

Diffuse Reflectance IR Fourier Transform Spectroscopy (DRIFTS)

Samples were conditioned to ambient temperature and humidity. (Attempts to control the environment within the spectrometer were unsuccessful.) A background of finely ground potassium bromide was used in a diffuse reflectance accessory made by Spectra-Tech. No blockers or filters were used. 400 scans were taken over a range

* XFIX is part of the CCP13 software suite.

between 4000 and 750 cm^{-1} at a resolution of 4 cm^{-1}. Sample height was modified for each set of samples so that the maximum reflectance (observed at approximately 3800 cm^{-1}) registered approximately 120%. This maximized the signal to noise ratio at low reflectance. Each individual sample was scanned at least 5 times in different locations to average out the effects of local structure.

The group of absorption bands in the region between 1200 and 1400 cm^{-1} is related only to crystallinity[9] following the method of Nelson and O'Connor[10] the ratio of the area of the band at 1372–1375 cm^{-1} (C—H band) to the relatively constant C—H stretching band at 2900 cm^{-1} was taken as a measure of the crystallinity. Following the method of O'Connor,[11] the ratio between the CH_2 scissoring peak at 1429 cm^{-1} and the hydrogen bonding peak at 898 cm^{-1} was calculated to give a measure of hydrogen bonding.

Water Retention Values

Paper samples were soaked in distilled water for at least an hour prior to being centrifuged at 3000 *g* to remove surface water. Development of this procedure is explained later in the Discussion. A 50 mesh wire screen at the bottom of each tube enabled water to drain. Four 5 min cycles were used. The wet samples were then weighed. After drying in an oven at 105°C for at least an hour, as specified by Technical Association of the Pulp and Paper Industry (TAPPI) standard T412 om-94, the samples were weighed again. The loss in weight is representative of the weight of water taken up by swelling: final results are expressed as the ratio of grams of water imbibed per gram of sample. Because some evaporation is inevitable, reported water retention values (WRV) results are expected to underestimate the actual amount of water absorbed.

Tensile Testing

A Pulmac TS-100 pneumatically operated tester was used to perform a zero span tensile test according to TAPPI classical method T 231 cm-96 in which a paper sample is clamped between two jaws that are in initial contact and are then pulled apart at a uniform rate. Sample size was 20 × 90 mm, which was wider than the clamping jaws to ensure that the fibers under test were uniformly clamped across the jaw width and eliminate edge effects. At least ten replicates were performed for each condition. Units of zero span tensile strength used in this work are kg/15 mm, where 15 mm is the width of the jaws.

Wide span tensile tests were conducted at a constant rate of elongation of 25 mm/min over an initial gauge length of 100 mm. The samples were 25 × 150 mm in size, cut so that the long direction was parallel to the paper's machine direction. Samples were cut using a paper cutter but may not have all been within the TAPPI standard's specification of sides parallel within 0.1 mm. Samples that failed within 5 mm of the clamps were generally accepted as valid because the failure could not be attributed to faulty clamping and nearly always occurred with the most degraded samples. Units of wide span tensile (failure) strength reported in this research are *N*. Wide span results reported are the average of at least 5 valid samples.

Scanning Electron Microscopy

Samples were gold sputtered twice, with 180° rotation, and were observed at a magnification of 540×. Uncoated samples were also tested in tensile deformation *in situ* in an ElectroScan Environmental Scanning Electron Microscope (ESEM).

RESULTS

SAXS Analysis of Void Parameters in Filter Paper

Data collected at the Synchrotron Radiation Source are subject to errors, which can lead to results that appear to be consistent within a given trip but not with results obtained on a different trip. For example, the amount of parasitic scatter from the beam stop and detector characteristics may change and may not be wholly corrected. Reproducibility was of an acceptable standard: the majority of data points lie within one standard deviation of the mean despite the fact that the trips to Daresbury took place over a one-year period. The error bars in all the following data incorporate both the systematic errors arising from different trips and random errors within a single trip. The values of void parameters obtained will be subject to further systematic errors arising from inherent limitations in the analysis. This is discussed in more detail in the Discussion.

Figure 1 shows the radius of gyration obtained from filter paper. The dry radius of gyration remains fairly constant at approximately 140 Å. In

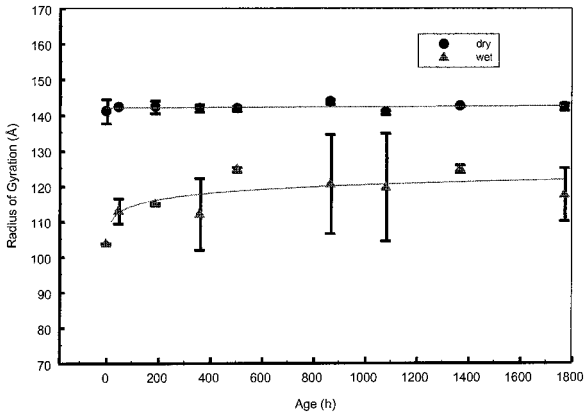

Figure 1 The radius of gyration of filter paper aged at 160°C *in vacuo*. The dry void size undergoes little change on aging, whereas the wet void size increases to approach dry values.

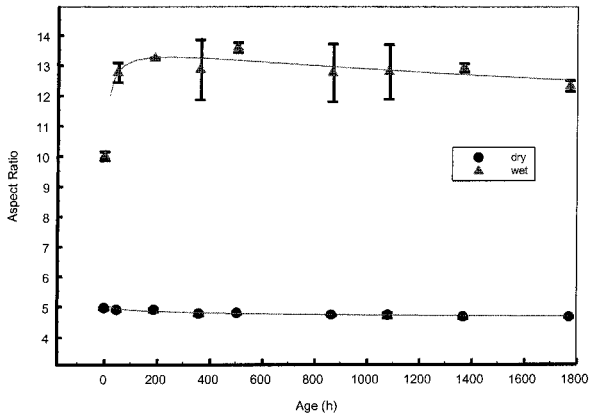

Figure 3 The average void aspect ratio of filter paper aged at 160°C *in vacuo*. Dry values change little, but the wet values undergo an initial increase followed by a small decline.

the case of wet material, the initially lower R_g of 105 Å increases with age to approach the constant dry value.

Figure 2 shows the average void area of aged filter paper. Overall, there is very little change in either the wet or the dry values of S_3. Values of S_3 in dry paper average 50,000 Å^2, corresponding to dimensions of roughly 100 by 500 Å (as determined by the aspect ratio calculations); wet values are somewhat lower at a consistent 15,000 Å^2, or approximately 40 by 370 Å.

Figure 3 shows the average void aspect ratio. The dry void aspect ratio shows little change with age, remaining fairly constant around 5. The void aspect ratio does show a trend with age in wet paper, however: it increases from the initial value of 10 to a final value of about 12.5 over several hundred hours, with the majority of the increase taking place within the first 200 h.

Figure 4 shows averaged values for the void fraction product in aged filter paper. The dry paper values do not show any visible trends with the majority of data points being on a straight horizontal line. Wet values, on the other hand, show a decrease in VFP to approach the dry values at greater age.

SAXS Analysis of Void Parameters in Ramie

The values for the radius of gyration for the oriented ramie samples represent the average

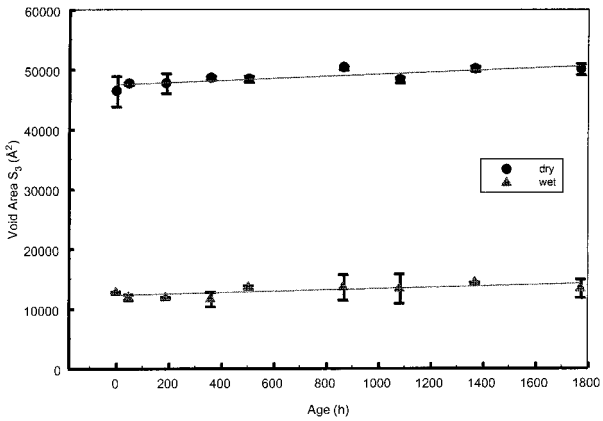

Figure 2 The void area of filter paper aged at 160°C *in vacuo*. Dry voids are larger than wet voids; the area is not strongly dependent upon aging time.

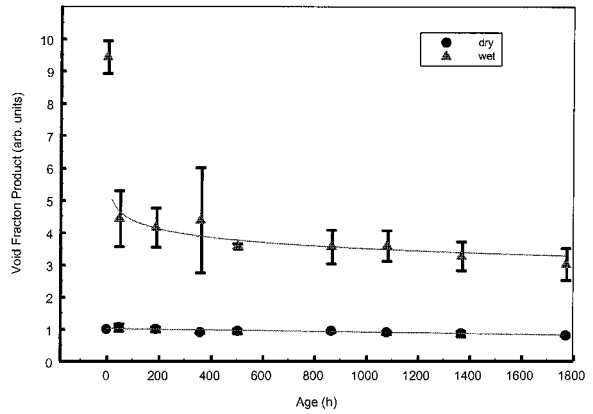

Figure 4 The void fraction product ($Q/\Delta\rho^2$) of filter paper aged at 160°C *in vacuo*. The number of voids hardly changes in dry aged paper but in wet material, the proportion of voids decreases significantly during the initial stages of aging.

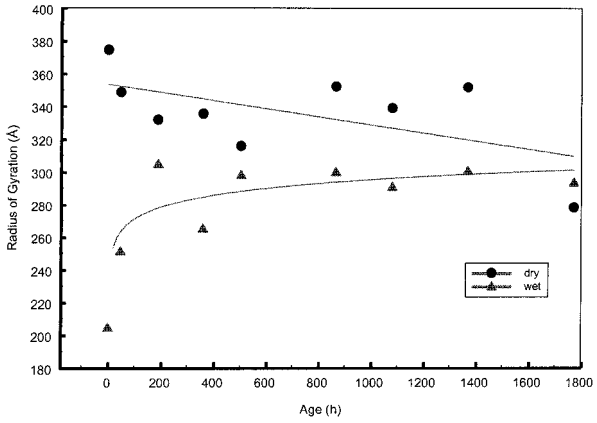

Figure 5 The radius of gyration of ramie aged at 160°C *in vacuo*.

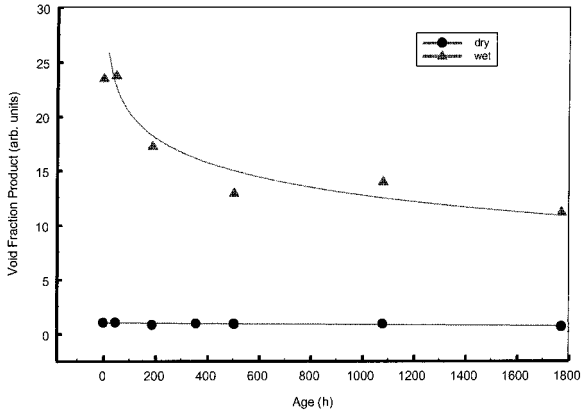

Figure 6 The void fraction product of ramie aged at 160°C *in vacuo*.

through a section perpendicular to the fibers axis, unlike paper, where the random orientation in the plane means that the measured R_g includes components from both the long and short axes of the void. They are all taken from data collected on the same trip: errors are assumed to be comparable to those reported for paper. Errors within these data, however, can be estimated by considering the values obtained by duplicate scans of dry and wet as received ramie. The average value for two replicates of dry as received ramie is 370 $\pm$ 4.2 Å (1% error). For three repeats of wet as received material, the average value is 200 $\pm$ 7.6 Å (4% error).

Figure 5 shows the radius of gyration of cross section obtained from ramie. The dry values decreased with age. This is contrast to the results obtained for paper, in which no change was seen. Trends in wet radius of gyration of aged ramie are similar to those given for paper. Initially lower than the dry values, the wet R_g increases with age to approach the dry.

Normalized and corrected experimental data for the void fraction product are shown in Figure 6.

Table I shows the results of the azimuthal scans of the SAXS data from ramie. Wet ramie has a consistently longer void length than dry ramie and there is no trend in void length with age. Taking the trend in void length together with the relative values of wet and dry void radius of gyration, it would appear that on wetting, the voids become longer and thinner. This agrees with findings for the aspect ratio of aged filter papers, which includes both the short and long void dimensions: on wetting, the aspect ratio doubles. The errors introduced by linear fitting can be substantial, despite high values of the linear correlation coefficient, so it is not surprising that no trends in either void length or misorientation were found with respect to sample age within the accuracy of the analysis.

Wide Angle X-Ray Scattering

WAXS crystallinity data for dry filter papers aged are presented in Figure 7. Errors between replicate samples are also less than 1%.

DRIFTS

Reproducibility in DRIFTS results was found to be acceptable. There was no appreciable error introduced by scanning different regions of the same sample, or different samples of the same age. The IR crystallinity is shown in Figure 8.

Table I Calculated Void Misorientation B_ϕ and Length L_3 for Ramie Aged at 160°C *in vacuo*[a]

Sample	Age (h)	B_ϕ (rad)	L_3 (Å)	R^2
Dry	0	0.839	196	0.950
	47.25	0.800	140	0.974
	187.75	0.837	117	0.986
	503.5	0.868	139	0.593
	1772.25	0.656	120	0.985
Wet	0	0.866	242	0.943
	47.25	0.938	270	0.999
	187.75	0.796	240	0.997
	503.5	0.872	x	0.976
	1772.25	0.766	275	0.862

[a] The wet void length at 503 h could not be calculated as there was a negative intercept.

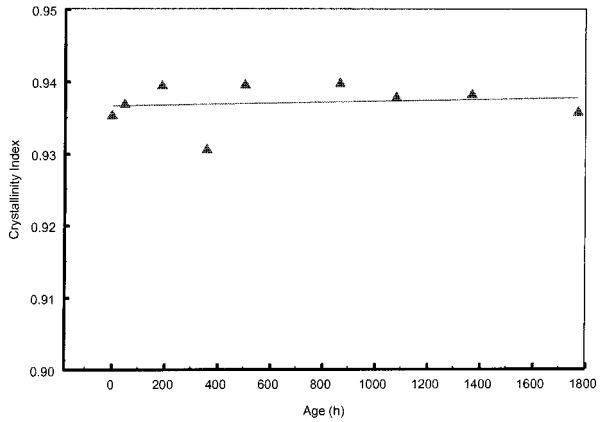

Figure 7 WAXS crystallinity index in dry filter paper aged 160°C *in vacuo*. There is no significant change in crystallinity, implying that no large scale variations in ordering occur on thermal aging.

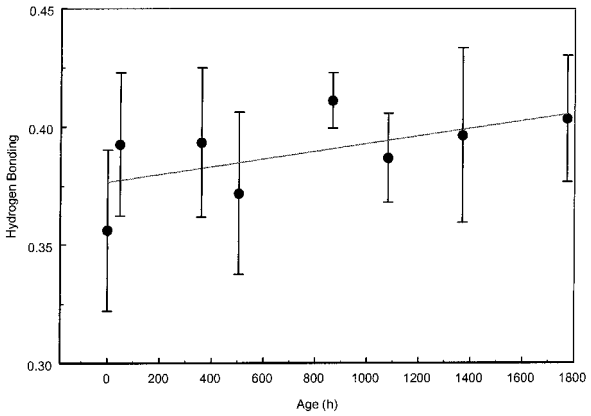

Figure 9 Changes in hydrogen bonding with age in filter paper aged at 160°C *in vacuo*. Even at these conditions, there is no significant trend. The slight increase in hydrogen bonding, however, is not supported by an increase in IR crystallinity. This may not necessarily indicate that no changes in hydrogen bonding occur, as there is an already high level of "background" hydrogen bonding in cellulose, so small changes may not be detectable.

Figure 9 shows the change in hydrogen bonding as a function of age.

Water Retention Values

Two sample weight ranges, 1 and 0.4 g, were used to determine if water retention was proportional to the amount of material used. If so, the amount of water retained by the samples would be inversely correlated to the surface area, with larger amounts of sample yielding larger WRV values. The effect of the number of 5 min centrifuging cycles was also investigated, to a maximum of six cycles. The results of this investigation are shown in Figure 10. It is apparent that the concurrence of WRV values obtained from both sample weight ranges is identical. This is reassuring because it demonstrates that the WRV is independent of the surface area and hence that the centrifuge is effectively removing surface water in the weight range used. The effect of increasing the number of centrifuging cycles is also visible in the figure. The largest decrease in WRV occurs within the

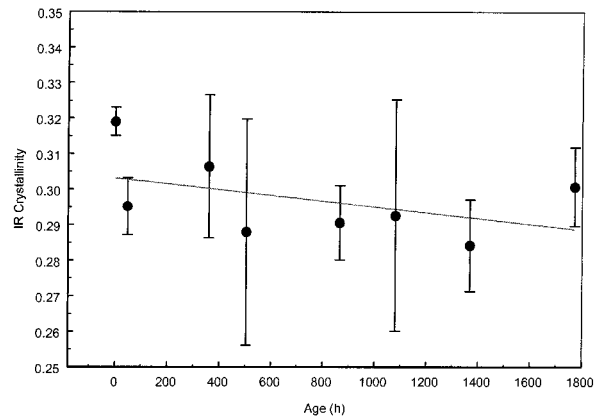

Figure 8 IR crystallinity changes in filter paper aged at 160°C *in vacuo* as calculated using the method of Nelson and O'Connor. As with the WAXS results, there is no change in crystallinity in spite of marked changes in SAXS parameters and mechanical strength.

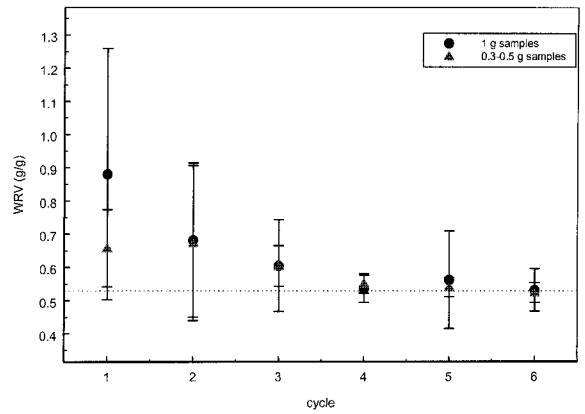

Figure 10 The effect of sample weight and number of centrifuging cycles on the calculated water retention value of as received filter paper. Each point is the result of at least 8 replicates. Based on these results, it was concluded that WRV is independent of sample weight in the range between 0.4 and 1 g, and that 4 cycles was the optimum number to use.

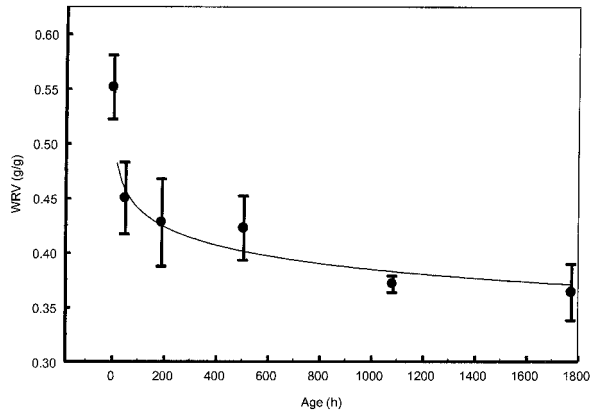

Figure 11 Water retention values for aged filter paper. Data points represent the average of four replicates. As with other physical parameters monitored in this work, the largest changes are apparent in samples aged at 160°C in air.

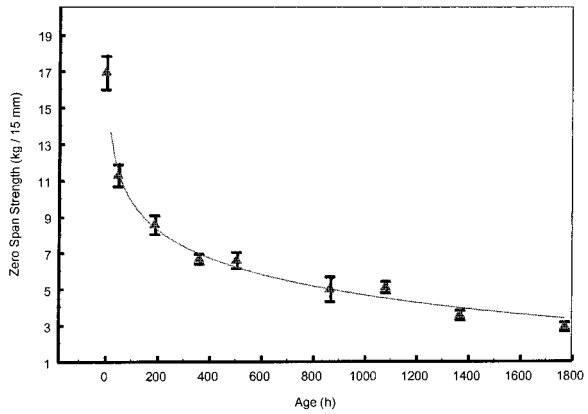

Figure 12 The zero span tensile strength of aged filter papers. Reproducibility is quite good, as shown by the relatively small error bars and the similarity of values for as received material.

first three cycles, implying that an appreciable amount of water is still being removed. Whether to take the results after 15 min (3 cycles) as in the procedures of Matsuda[8] and Weise[9] or 20 min (4 cycles) was decided based on the standard deviation of the results: it is consistently smaller after four cycles. Also, the decrease in WRV between cycles 4 and 5 (and 5 and 6) is small compared to between cycles 3 and 4. The drop in the former is likely to be attributable to evaporation rather than loss of surface water in the latter.

Figure 11 shows the WRV values using four cycles and samples of weight between 0.3 and 0.5 g. It is clear that the WRV value falls with age over similar time scales to the changes in radius of gyration and void fraction parameter.

Tensile Testing—Zero and Wide Span

Figures 12 and 13 show the zero and wide span tensile strength of the filter paper samples. Both parameters fall over similar time-scales to the changes in WRV, radius of gyration, and void fraction parameter.

SEM

Figures 14 and 15 show the failure zones of as-received filter paper, and filter paper aged in air. In the unaged material, fibers exhibit fibrillation and pull out rather than break, whereas in the aged material a straight failure zone is seen.

Environmental scanning electron microscopy allowed the fracture process to be observed *in situ* under low vacuum conditions. This avoids the need for gold sputter coating of the samples and enables dynamic images to be collected. As-received and aged samples were notched such that tensile failure would be induced in a narrow zone. As the samples were pulled apart, it was clearly seen that the as-received fibers pulled out from the fibers network on opposite sides of the failure zone: previously interleaved fibers were pulled past each other, leaving each side of the failure

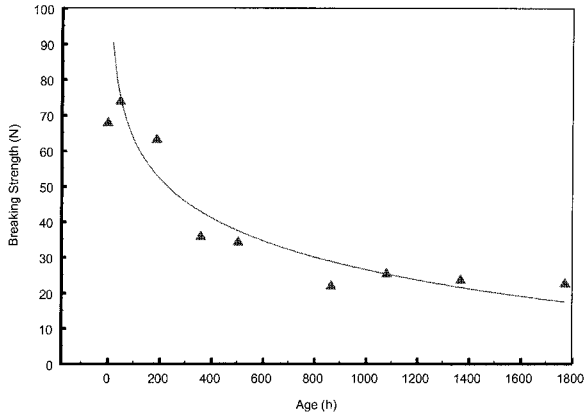

Figure 13 The wide span tensile strength of aged filter paper shows a similar trend to that of zero span strength in Figure 10 Wide span strength is a reflection of both fibers and interfiber bond strength. Reproducibility is not quite as good as the zero span condition because of the larger gauge length of material tested. Random flaws, edge effects, and similar millimeter to centimeter scale features can adversely affect strength; these are not influential in zero span strength. Error bars were not available for all samples.

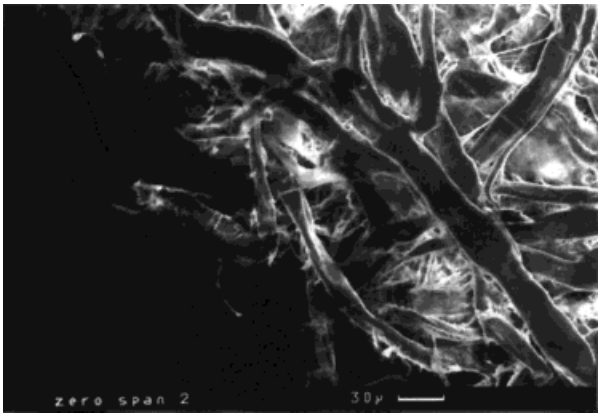

Figure 14 The failure zone of as-received filter paper. The fibers have been pulled out to some degree (shown by the ragged fracture edge) and fibrillation is visible.

zone with an irregular profile. Aged fibers, on the other hand, appeared to snap across the failure zone rather than pull out, leaving a relatively straight failure path. These observations support those from conventional SEM.

DISCUSSION

Guinier Analysis—Approximations and Applicability

Guinier analysis is only an approximate method of characterizing the SAXS scatter obtained. First, the product $q_{\max}R_g$ is in excess of the value at which the intensity begins to deviate from the Guinier approximation, where $q_{\max}$ is the maximum value of q used in the extrapolation. If homogeneous one-dimensional rod scatterers are assumed, the critical value of $q_{\max}R_g$ is 0.7; for spheres, the value is 1.69.[12] For the paper samples with the angular range available, the actual value of $q_{\max}R_g$ ranges between 0.81 and 1.7. A similar analysis applied to the radii of gyration of cross section in ramie also gives $q_{\max}R_g$ values outside the ideal range. Second, the dilute system assumption is not valid in wet samples, although this effect is reduced by the random size distribution of voids. These two factors mean that the R_g and S_3 values derived will depend on the angular range used to calculate them and must not be treated as being absolutely correct. The values obtained are likely to be an underestimate. However, the observed trends were found to be largely independent of range used.

In this work, a cellulose fibers is assumed to be a two-phase structure with a continuous phase of cellulose (amorphous and crystalline cellulose are counted as one phase) and a discontinuous void system within each fibers. The voids, either air filled or water filled, are assumed to be the scattering bodies. In paper samples, the radius of gyration is a measure of their cross sectional void size because the fibers all lie randomly oriented in approximately the same plane. As a result of the scattering geometry, all paper void parameters represent the average over three orthogonal dimensions. This is the result of the paper fibers being randomly oriented in two dimension in a plane perpendicular to the incident beam. In ramie samples, Guinier analysis yields a radius of gyration of cross section in the plane perpendicular to the fibers axis.

The Effects of Hydration on Void Structure in Filter Paper and Ramie

Table II summarizes the changes in structure in unaged ramie and in filter paper on hydration. The radius of gyration decreased when water was added to the structure and void area was reduced. Also notable is the drop in void fraction product between wet and dry material. However, the aspect ratio is higher in wet rather than dry. This can be interpreted as being indicative of fibril separation by water to open many new, smaller voids at the expense of the much larger original voids: more scattering is observed at higher angles in wet samples, implying smaller structures.

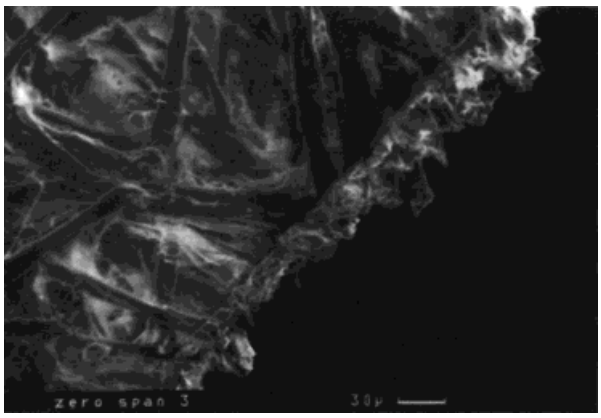

Figure 15 The failure zone of filter paper aged at 160°C in air. The mode of fiber failure appears to be brittle, as there is little fibrillation and the fracture edge is well defined. Note that one fiber has broken at an angle.

Table II Summary of Changes in Unaged (a) Filter Paper and (b) Ramie on Wetting

(a) Parameter	Dry	Wet
Radius of gyration (Å)	140	105
Void area (Å^2)	50,000	13,000
Void fraction product (au)	1	~ 8
Aspect ratio (rectangle)	5	10
Void dimensions (Å)	480 × 100	370 × 40
(b) Parameter	**Dry**	**Wet**
Radius of gyration of cross section (Å)	380	200
Void fraction product (au)	1	~ 25
B_f	0.84	0.85
Void length (Å)	200	250

The formation of new voids is supported by the significant increase in the void fraction product in wet samples.

The Effect of Thermal Aging on Void Structure in Filter Paper and Ramie

The basic trend in R_g, visible to an increasing extent as aging progresses in both paper and ramie, is for the wet values to approach dry values. This is mirrored by a fall in wet void fraction product, which approaches dry values with age. Together these two parameters imply that on wetting, voids are smaller and more numerous, but on aging the ability to form new voids is inhibited. This results in an increase in the average void size and a fall in the invariant as the structure becomes dominated by preexisting (dry) voids. The average void sizes in paper (averaged over three dimensions) are shown in Figure 16, assuming rectangular voids for ease of drawing. Aging results in voids with increasing wet aspect ratios. Wet void parameters therefore show trends on aging consistent with a reduction in the ability of water to penetrate and expand the cellulose structure.

The void parameters of dry paper describe a structure with large and relatively few voids and show no trends with age. Any structural rearrangements must be either at the crystallite length scale (i.e., of the order of 10 Å) or at many hundreds of angstroms, too large to be resolved. A small decrease was seen in the radius of gyration of cross section of the dry ramie fibers.

Ramie shows greater percentage changes than paper. There are several possible explanations for this. First, the ramie data extended to lower scattering angle and hence includes information from larger length scales (experimentally, $q_{\min}$ was 0.005 Å^{-1} for ramie, 0.0115 Å^{-1} for paper). Second, the accessibility to the cellulose of the ramie fibers is greater than in paper so degradation may be facilitated. Third, the orientation of ramie might allow structural changes to be more easily seen because the section across which the radius of gyration is taken is limited to the plane perpendicular to the fibers axis. The R_g values of paper are averages for the entire void, including the long axis, which might mask smaller scale changes.

The Effect of Thermal Aging on Crystallinity and Hydrogen Bonding in Filter Paper

WAXS crystallinity values of just over 90% for unaged filter paper were obtained: these are the same order of magnitude as those reported in the literature (e.g., ref. 13). No change within the uncertainty of measurement was observed.

Cellulose crystallinity as calculated by IR methods is also unchanged with age. Quantitative agreement of IR crystallinity with WAXS

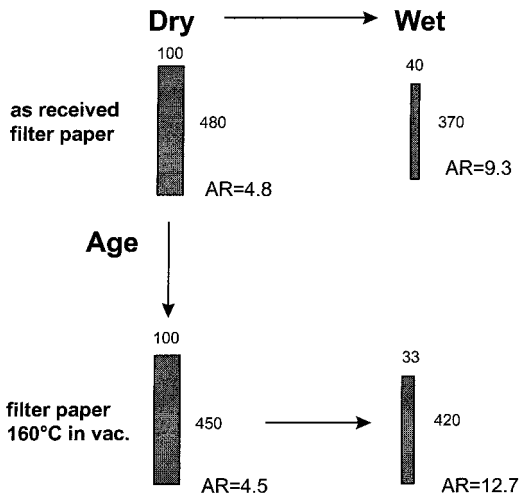

Figure 16 Approximate rectangular void dimensions (in Å) as determined by the void area and aspect ratio. More credence should be given to the trends rather than the values given. There is evidence for the voids becoming smaller and having a larger aspect ratio on wetting, but no definite changes are apparent after aging at 160°C *in vacuo* for over 1000 h. Typically, the void aspect ratio increases with aging in other samples.

crystallinity is not to be expected as the two methods use different criteria to define crystallinity. The crystallinities are significantly lower than the values in excess of 50% reported by Nelson and O'Connor,[10] despite their use of milled cotton cellulose, which should have less ordering than native fibers. There is a possibility of systematic error in the values introduced by the fact that the samples were not dispersed. There is disagreement in the literature regarding what in direction, if any, the crystallinity of cellulose changes with aging so these results are not anomalous.[13,14]

Hydrogen bonding as indicated by DRIFTS also remained unchanged on aging. That there is no significant variation in these parameters may not necessarily preclude changes. There is already a large amount of crystallinity and hydrogen bonding in as-received cellulose so if the changes induced by aging are relatively small, they will be swamped out by the high level of background.

The Effect of Thermal Aging on Water Retention Values in Filter Paper

The decrease in water retention value after aging is consistent with changes in the SAXS void parameters, which suggested that water was less able to penetrate the fibers on aging.

The Effect of Thermal Aging on Mechanical Failure

Previous work has shown that there is a strong correlation between loss of zero span tensile strength and the degree of polymerization.[3] Because the cellulose crystallites are the primary load-bearing component of fibers, reducing the degree of polymerization reduces the ability of the fibers to sustain tensile loading. The more gradual loss of wide span strength may suggest that interfibers bond strength either increases or stays the same.

There are two different failure mechanisms observed for the as received and aged papers by SEM and ESEM. In the unaged material, fibers exhibit fibrillation and pull out rather than break. This implies that fibers strength is greater than interfibers bond strength. In contrast, the straight failure zone of aged material shows that the fibers are the weaker components. Lack of fibrillation may also imply increased interfibril bonding within a single fibers, which holds the fibrils together and results in a tighter structure.

These observations may be broadly described by three mechanisms: the fibers strength decreases, the interfibers bond strength increases, or both may happen simultaneously. That the zero span strength decreases with increasing age implies that fibers strength decreases. Well-documented decreases in the degree of polymerization of aged celluloses supports this.[3,15,16] There could be an increase in interfibers bond strength with age, but that the overall mechanical strength of paper is much lower in the regime of fibers failure compared to the increased strength when failure occurs by fibers pull out favors a loss of fibers strength to be the dominant mechanism.

It is widely accepted that chain scission is responsible for the loss of fibers strength in aged cellulose. However, it cannot be used to explain the loss in the ability of the fibers to hold water. To explain this, structural changes need to be considered.

Water as a Structural Probe

Water has been used in this work as a structural probe, as changes in cellulose–water interactions with aging may reveal modifications in structure. Because small changes are seen in dry samples as well as wet, there must be modifications in structure that occur independently of the presence of large amounts of water. It is well documented that the degree of polymerization of aged cellulose decreases with age. However, reducing the chain length is insufficient to explain all observations. Lower degree of polymerization (DP) may explain the loss in mechanical strength and the results seen using scanning electron microscopy but cannot account for changes in hydration. If it were simply a case of chain scission, wetting a highly degraded sample might cause it to absorb more water, not less, as it would be expected to be physically unable to hold itself together.

That the ability to hydrate decreases with age implies that water is unable to expand the structure. What mechanism is likely to be responsible? It is well known that cellulose has a high degree of hydrogen bonding, possibly as high as 100% in dry material.[17,18] Cellulose is also highly crystalline. If water is to penetrate the structure, it can enter preexisting capillaries between microfibrillar elements of cellulose in the dry fibers or form its own capillaries by separating previously bonded surfaces.[19] Less ordered material is easier to separate because the hydrogen-bonding environment is less regular. If given the opportunity, the cellulose

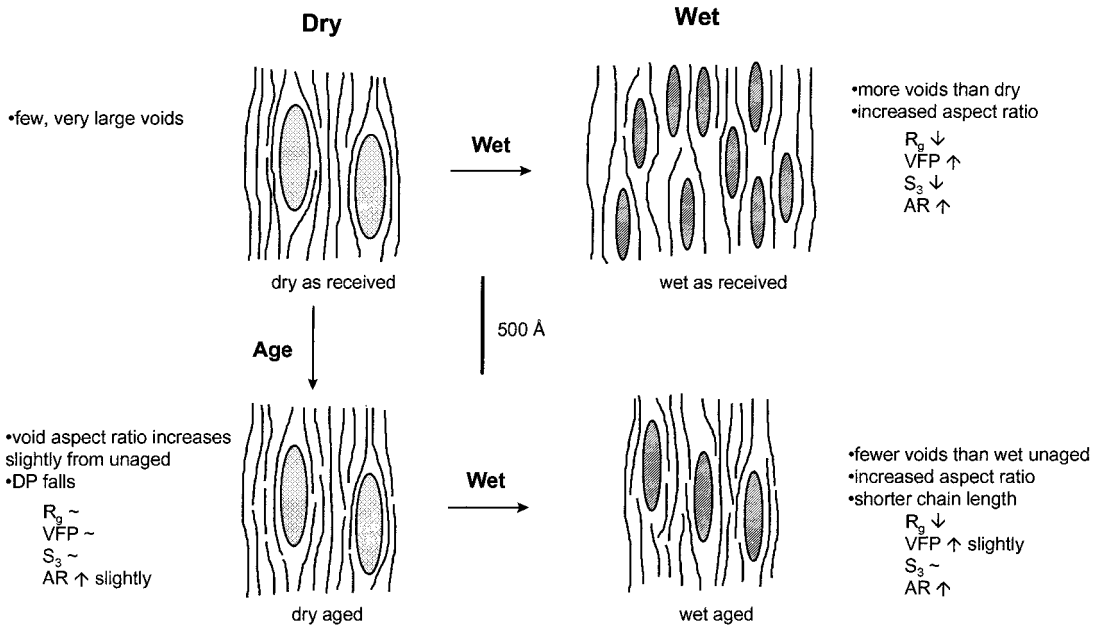

Figure 17 An approximate representation of the changes occurring in void dimensions and distribution in cellulose on wetting and aging. Although the absolute values quoted are not reliable, the trends are believed to be accurate. Trends are reported with respect to dry as received material.

structure will tend toward a lower energy state by perfecting interfaces and increasing order. This suggests that H bonds will be reallocated such that a crystalline structure is approached. As ordering increases, it becomes more difficult for water to enter and expand the structure. Changes in hydrogen bonding will be hard to monitor owing to the high background level; large changes in crystallinity will not be apparent since small rearrangements are envisioned. This view, that modifications to the internal H-bonding environment are responsible for changes in hydration behavior, is supported by the weight of indirect evidence arising from work on hornification[20,21] (reviewed in ref. 22). It is also consistent with aging models, which suggest improved crosslinking as an explanation. As no evidence for additional covalent bonding has been found, these crosslinks are most likely to be hydrogen bonds.

In hornification, free water provides cellulose chain mobility and breaks H bonds. On drying, the broken bonds re-form such that the resulting structure is more ordered, compact, and tightly bound. The material becomes stiffer and has lowered swelling ability. It is possible that elevated temperature provides adequate mobility for chain segments and allows H-bond reallocation, and that heat is an analogue for free water. Higher temperature will plasticize cellulose, which makes chain rearrangements easier. The decrease in DP with age further facilitates possible rearrangements. The conditions of accelerated aging will also comprehensively dehydrate the sample. Thus, conventional hornification may be partially or fully responsible for the changes. Notwithstanding the lack of large amounts of water in thermal aging, the similar trends in water retention value in aged or hornified cellulose suggests a similar underlying mechanism independent of the degree of polymerization.

Structural Model of Thermally Aged Cellulose

Based on the findings summarized above, a tentative model depicting structural changes on aging in cellulose is now presented. This is given in Figure 17. Dimensions in the figure are approximate: less reliance should be placed on the absolute values rather than the relative changes between the different conditions, particularly aspect ratio and number of voids. In dry, unaged material, there are few, relatively large voids. On wetting, this void structure is disturbed by water, which forms smaller, more pointed voids in between the microfibrils: water acts as a medium for chain movement and disrupts the original interfibril hydrogen bonding. The number of voids increases on wetting as shown by an increase in the void fraction product and water retention value.

On aging, the degree of polymerization of the cellulose is reduced. It is also likely that small rearrangements between adjacent microfibrils increase the degree of structural perfection. The voids in the dry state do not change very much, although the aspect ratio may decrease slightly. On wetting aged cellulose, the structure does not expand to the same extent as in the unaged material, as the void fraction product only increases slightly. The difference between the measured R_g in dry and wet samples becomes smaller as the paper is aged, supporting this view. This is in spite of the lower DP which might be expected to reduce structural integrity, thereby making it easier to form additional or larger voids.

Relating Structural Changes to Mechanical Properties

Can structural changes on aging be related to overall properties? A relationship certainly exists between aging conditions and retention of zero span (i.e., fiber) strength, which means that the change in structure brought about by a loss of DP can be related to a macroscopic property. It is less obvious how changes in void structure might influence mechanical strength. As a result, it is difficult to assert if a direct relationship exists between the structures in cellulose at ångstrom and millimeter scales. At larger scales in paper, the influence of microstructure on overall strength is even less clear as the effects of mass distribution and interfibers bonding become important. The inability to draw together age-related modifications in microstructure to larger scale mechanical properties means that, for the purposes of the structural model proposed, the two scales can only be viewed in isolation.

CONCLUSIONS

In the literature, loss of swelling ability is correlated with partial or complete drying of cellulose fibers, and is explained by an increase in nonreversible intercellulosic hydrogen bonding, resulting in adhesion of cell wall lamellae. The present results demonstrate that increased aging, that is, increased degradation, also leads to similar effects as hornification. It is reasonable to surmise that similar mechanisms may be involved in both thermally accelerated aging and hornification with respect to hydrogen-bond formation and loss of swelling ability. However, the changes in mechanical properties and fibers strength are likely to be largely a consequence of chain scission rather than the changes in the void structure.

One of us (KLK) is grateful to both the Commonwealth Scholarship Commission in the United Kingdom and the Natural Sciences and Engineering Research Council of Canada for financial support of this research. Prof. M. T. Kortschot and Prof. Emeritus D. A. I. Goring of the Pulp and Paper Centre, University of Toronto, are thanked for useful discussions and for use of testing facilities. Dr. A. E. Emsley and R. Heywood of the Department of Chemistry, University of Surrey, provided samples and performed some aging experiments. The assistance of the station scientists at the Daresbury Laboratory (Dr. B. U. Komanschek, Dr. A. Gleeson, and S. Slawson) is gratefully acknowledged.

REFERENCES

1. Kato, K. L.; Cameron, R. E., submitted.
2. Roberson, D. D. Tappi 1976, 59, 63.
3. Zou, X.; Gurnagul, N.; Uesaka, T.; Bouchard, J. Polym Deg Stab 1994, 43, 393.
4. Emsley, A. M.; Stevens, G. C. Cellulose 1994, 1, 26.
5. Shioya, M.; Takaku, A. J Appl Phys 1985, 58, 4074.
6. Ruland, W. J Polym Sci 1956, 22, 385.
7. Wang, W.; Ruland, W.; Cohen, Y. Acta Polym 1993, 44, 143.
8. Segal, L.Text Res J 1959, 29, 786.
9. Nelson, M. L.; O'Connor, R. T. J Appl Polym Sci 1964, 8, 1311.
10. Nelson, M. L.; O'Connor, R. T. J Appl Polym Sci 1964, 8, 1325.
11. O'Connor, R. T.; DuPre, E. F.; Mitchum, D. Text Res J 1958, 28, 382.
12. Guinier, A.; Fournet, G. Small Angle Scattering of X-rays; Walker, C. B., Tr.; Wiley: New York, 1955.
13. Safy el Din, N. M.; Fahmy, A. M. Polym Intl 1994, 34, 15.
14. Major, W. D.Tappi 1958, 49, 530.
15. Du Plooey, A. B. J. APPITA 1981, 34, 287.
16. Shafizadeh, F. In Cellulose Chemistry and Its Applications; Newell, T. P., Zeronian, S. H., Eds.; Chichester: Ellis Horwood, 1985; p 266.
17. Eillis, J. W.; Bath, J. J Am Chem Soc 1940, 62, 2859.
18. Scallan, A. M. Trans BPBIF Symp 1977, 1, 9.
19. Stone, J. E.; Scallan, A. M. Trans BPBMA Symp1965, 1, 145.
20. Weise, U.; Maloney, T.; Paulapuro, H. Cellulose 1996 3, 189.
21. Laivins, G. V.; Scallan, A. M. Products of Papermaking, 10th Fundamantal Research Symposium; Baker, C. F., Ed.; Oxford: Pira International, 1993; Vol 2, p 1235.
22. Kato, K. L.; Cameron, R. E. Cellulose, in press.